

# Planning coordinated motions for tethered planar mobile robots

Xu Zhang<sup>1</sup>, Quang-Cuong Pham<sup>1,\*</sup>

Singapore Centre for 3D Printing, School of Mechanical & Aerospace Engineering,  
Nanyang Technological University, 50 Nanyang Avenue, 639798, Singapore

## Abstract

This paper considers the motion planning problem for multiple tethered planar mobile robots. Each robot is attached to a fixed base by a flexible cable. Since the robots share a common workspace, the interactions amongst the robots, cables, and obstacles pose significant difficulties for planning. Previous works have studied the problem of detecting whether a target cable configuration is intersecting (or entangled). Here, we are interested in the motion planning problem: how to plan and coordinate the robot motions to realize a given non-intersecting target cable configuration. We identify four possible modes of motion, depending on whether (i) the robots move in straight lines or following their cable lines; (ii) the robots move sequentially or concurrently. We present an in-depth analysis of *Straight & Concurrent*, which is the most practically-interesting mode of motion. In particular, we propose algorithms that (a) detect whether a given target cable configuration is realizable by a *Straight & Concurrent* motion, and (b) return a valid coordinated motion plan. The algorithms are analyzed in detail and validated in simulations and in a hardware experiment.

*Keywords:* multi-robot motion planning, tethered robots

## 1. Introduction

In many applications, tethers are used to provide power and resources to robots or used as a communication link [1, 2, 3], especially in extreme environments, such as in underwater, disaster recovery and rescue [4, 5, 6]. While tethering helps in communication and resource delivery, it also poses challenges to robot control and planning. The limited-length cable restricts the mobile robot to the workspace around its home station. In addition, due to the presence of obstacles and cables, certain positions can be reached by robot only under specific robot cable configurations. Under many circumstances, multiple tethered robots have to cooperate and work together in a shared workspace [4, 5, 7, 3], which introduces more constraints to the planning and control problems. More specifically, in the large-scale, multi-robot 3D Printing system [3], the tethers are indispensable to deliver the fresh concrete from the mixer to the print nozzle. Consider also the cable-cable interaction and robot-cable interaction when multiple tethered robots are deployed for terrain and harsh environment exploration [4, 5, 7]. It is important to make sure that the cables are not entangled while the robots move to their target positions, considering the above mentioned interactions and obstacle avoidance.

Here we consider multiple tethered planar (point) mobile robots sharing a common workspace. Each robot is attached to a fixed base by a flexible cable, which is kept taut at all times. The cable can be pushed by other robots, and can bend around other robots or obstacles. The assumptions are consistent with the requirements of the tethers in many

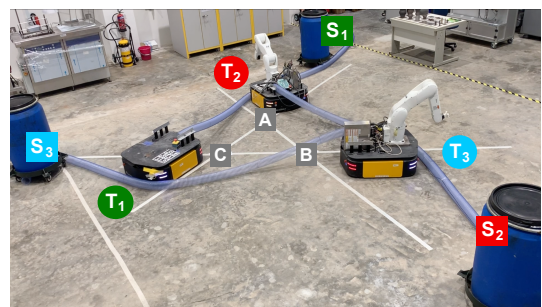
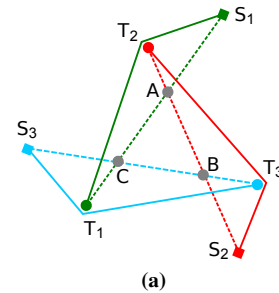


**Fig. 1.** An example of coordinated motion planning problem for three tethered mobile robots. (a) Each robot  $r_i$  ( $i = 1, 2, 3$ ) must move from its starting position  $S_i$  towards its target position  $T_i$ , while being tethered to  $S_i$ . The desired configuration of the cables at the end of the motions are depicted in solid lines. This paper proposes an algorithm to plan simultaneous, straight-line, motions of the robots to realize the desired cable configuration. We show in particular that the motion priority at the intersection points  $A, B, C$  is critical. (b) Hardware implementation of the coordinated motion. See full video of the experiment at <https://youtu.be/Wdk9E0bB4yA>.

\*Corresponding author. Email: cuong@ntu.edu.sg.

practical applications, such as the material-delivery tethers in the concrete 3D Printing system [3], or in terrain explorer system [7]. Previous work has studied the problem of detecting whether a target cable configuration is intersecting (or entangled) [8]. Here, we investigate the *motion planning* problem to *realize* a given non-intersecting target cable configuration. More precisely, we study four possible modes of motion – Straight/Sequential and Straight/Concurrent, Bent/Sequential, Bent/Concurrent, depending on whether (i) the robots move in straight lines or following their cable lines; (ii) the robots move sequentially or concurrently.

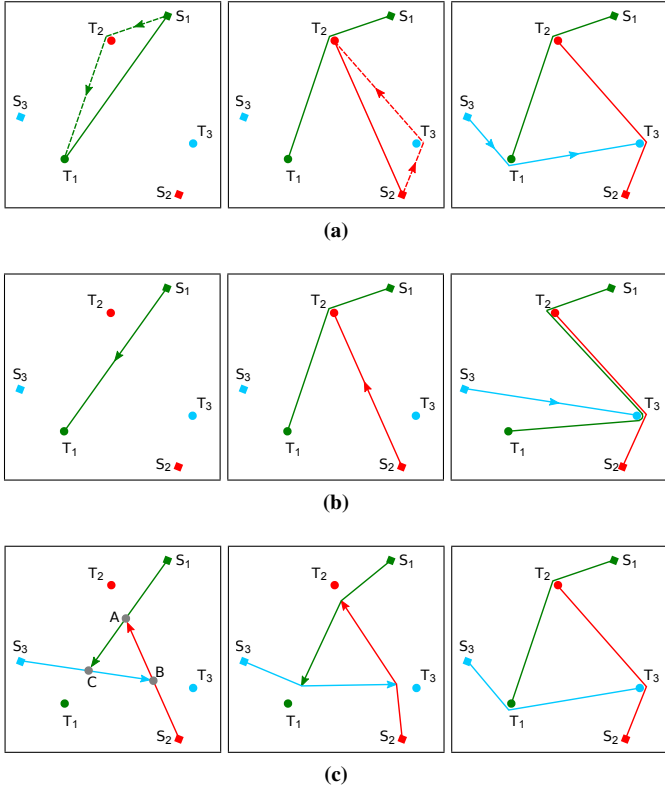


**Fig. 2.** An example of planning for a target cable configuration by different modes of robot motion. (a) *Bent/Sequential* mode. The target cable configuration can be achieved when robots move in the order:  $r_1$ ,  $r_2$  and  $r_3$ . Dotted cable lines retract to solid ones since the cables are kept taut at all times. (b) *Straight/Sequential* mode. The target cable configuration *CANNOT* be achieved by this mode of motion. The example shows how the final result deviates from the target cable configuration. (c) *Straight/Concurrent* mode. The target cable configuration can be achieved when robots move along the  $(S_i, T_i)$  straight-line segments at the same velocity.

### 1.1. Illustrative example

To illustrate some of the difficulties, consider a scenario with three tethered robots as in Fig. 1: each robot  $r_i$  ( $i = 1, 2, 3$ ) tethered to its starting base  $S_i$  must navigate from  $S_i$  to its target position  $T_i$ . The target cable configuration as shown in solid lines has to be achieved upon arrival of all robots.

In *Bent/Sequential* mode, the target cable configuration can be achieved, for example, in the order:  $r_1$ ,  $r_2$  and  $r_3$ . Since the cables are kept taut at all times, when  $r_1$  first moves along  $S_1 - T_2 - T_1$ , its cable  $C_1$  retracts to the straight-line segment

$S_1T_1$  when it reaches  $T_1$ . Then  $r_2$  moves along  $S_2 - T_3 - T_2$ , pushing cable  $C_1$  to the layout  $S_1T_2T_1$  as it reaches  $T_2$ , and  $C_2$  retracts to  $S_2T_2$ . Finally  $r_3$  moves along  $S_3 - T_1 - T_3$  and pushes cable  $C_2$  to the layout  $S_2T_3T_2$ . Since  $r_1$  has already arrived at  $T_1$ , cable  $C_3$  will bend around it and remain at its final layout as  $S_3T_1T_3$ . The target cable configuration is thus achieved (see Fig. 2(a)). Note that the configuration can also be achieved by *Bent/Concurrent* mode where the robots move simultaneously following their cable lines.

However, simply following robots' cable lines is not the most desirable motion scheme. Compared to *Bent* motion, *Straight-line* robot motion offers the following benefits:

- 1) *Straight-line* robot motion reduce traveling distance, which in turn improves time and energy efficiency. Take the two target cable configurations provided in this paper for example. To achieve the target cable configuration in Fig. 1 and Fig. 7(a), straight-line robot motion saves respectively 30% and 20% of the traveling distance compared to robot motion that follows cable lines.
- 2) It is well-known that in robot localization, rotational and curved translational motions induce larger estimation errors than straight motions, in relation to both Inertial Measurement Unit (IMU) and odometry [9]. Thus, by using the *Straight* mode, one can significantly reduce localization errors;
- 3) Working environment safety could be enhanced as straight-line robot motion is more predictable for the workers who need to collaborate or work in the same environment with the robots;

The first benefit motivates the work by Hert and Lumelsky [10], where an algorithm is proposed for robots to achieve a given target cable configuration by *Straight/Sequential* motion. *Straight/Sequential* mode improves the efficiency at the sacrifice of realizability, which is illustrated in Fig. 2(b). Suppose the robots move in the order of  $r_1$ ,  $r_2$  and  $r_3$  along  $S_1 - T_1$ ,  $S_2 - T_2$  and  $S_3 - T_3$  respectively. Upon arrival of  $r_1$  at  $T_1$  and  $r_2$  at  $T_2$ , we can obtain the same cable configuration as under *Bent/Sequential* motion, but after that,  $r_3$  must push  $C_2$  in order to navigate to  $T_3$ , which violates the target cable configuration, resulting in a deadlock. In their later work [11], *Straight/Concurrent* mode is considered, but the concurrent motions are not leveraged to solve deadlocks. Yet, considering again the example of Fig. 1, concurrency can be leveraged to solve the deadlock as follows:  $r_1$ ,  $r_2$  and  $r_3$  move along their  $(S_i, T_i)$  straight-line segments at the same velocity (see Fig. 2(c)). By doing so, they will indeed pass respectively points  $A$ ,  $B$  and  $C$  at the same time, which in turn satisfies the requirement that  $r_1$  passes  $A$  before  $r_2$  does,  $r_2$  passes  $B$  before  $r_3$  does, and  $r_3$  passes  $C$  before  $r_1$  does. The general algorithm to produce such a schedule is one of the main contributions of the present paper.

### 1.2. Contributions and organization of the paper

Our contribution in this work is three-fold. First, we systematically examine the realizability of a target cable configuration

by the above mentioned four modes of motion. We then present a further analysis of *Straight/Concurrent* motion, which is the most practically-relevant mode. Second, we propose algorithms to detect whether a given target cable configuration is realizable by *Straight/Concurrent* motion. Third, our algorithms return a valid coordinated motion plan if there exists a solution. In addition, we provide some corrections to the algorithms presented in [8] to detect whether a cable configuration is intersecting.

The remainder of this article is organized as follows. In Section 2, we review related works in motion planning for single and multiple tethered robots. In Section 3, we introduce the background on non-intersecting cable configurations, formulate the planning problem for multiple tethered robots, and survey the realizability of cable configurations by the four modes of motion. In Section 4, we present our planning algorithms for *Straight/Concurrent* robot motion in detail. In Section 5, we report experimental results in simulation and in hardware. Finally, we conclude our work in Section 6.

## 2. Related work

### 2.1. Single tethered robot

Motion planning for a single tethered robot mainly falls into two topics: 1) shortest path planning; 2) coverage and terrain exploration.

#### 2.1.1. Shortest path planning

There has been active research on planning the shortest path for a tethered robot to navigate from a starting position to a target position. Methods developed by Xavier [12] and Xu et al. [13] are similar: they construct a visibility graph based on the triangulation of the environment, and perform an almost-exhaustive enumeration of graph paths in the selected homotopy class. In [14, 15, 16], the authors approached the problem by using a conception of homotopy classes of the cables. The difference between these papers lies in the way they identify homotopy classes. Igarashi and Stilman [14] use distance from the initial vertex that entirely based on a metric, which under certain circumstances would fail to identify that two vertices in the graph represent two different homotopy classes. To avoid this failure, Kim et al. [15, 16] use a true homotopy invariant (h-signature) to construct a h-augmented graph that explicitly bears the topological information. The method is capable of producing an optimal result based on a discretized workspace. Similar concepts are also applied to plan for manipulation and transportation of objects on the plane using tethered mobile robots [17]. In another recent study [18] that is built on [15, 16], the authors use a visibility-graph based approach instead of the grid-based approach, and extend the point robot assumption to polygonal (translating) robot. Unlike prior work that generally adopts off-line global discretization of the configuration space, Teshnizi and Shell [19] decompose the environment into cells using a subset of the visibility graph. The approach enables dynamic generation of necessary parts of the space, which in

turn, improves efficiency of the proposed method. In their later work [20], they generalize the decomposition method to solve the planning problem for a robot attached to a stiff tether.

#### 2.1.2. Coverage and terrain exploration

Coverage and extreme terrain exploration have also been studied regarding planning for tethered robots. Shnaps and Rimon [21] present an online algorithm considering the case where a tethered robot has to cover an unknown planar environment that contains obstacles, and returns back to the base. Abad-Manterola et al. [22] give a motion planner for an *Axel* tethered robotic rover on steep terrains whose geometry is known a priori with high precision. Their work is later extended to the case where the terrain information is not fully known beforehand [23]. In [24], a nonvisual tether-based localization and mapping technique based on FastSLAM is developed and tested on the Tethered Robotic eXplorer (*Axel*). The online particle-filter approach is then expanded to TSLAM [25]. Using the same *Axel* platform with customized tether controller, the authors demonstrate visual route following for extreme terrain exploration [26]. Visual route following for a tethered mobile robot is also discussed in [27], without addressing tether management.

### 2.2. Multiple tethered robots

There are two major streams pertaining to multiple tethered robots planning: 1) cooperative control and manipulation; 2) navigation from respective starting to target positions.

#### 2.2.1. Cooperative control and manipulation

In [28], the authors propose a method that make multiple mobile robots accomplish tasks with the cables act as tools connected between the robots. Similarly, in [29], the authors address the cooperative control of two autonomous surface vehicles for oil skimming and cleaning.

#### 2.2.2. Robot navigation

Khuller et al. [30] plan for a team of robots to move from any starting location to any goal destination in a graph-structured space simultaneously while maintaining a particular configuration.

In some other applications, instead of keeping a particular formation, each of the robots needs to navigate to a different location for a specific task, where cable entanglement avoidance emerges as a crucial challenge. There are some remarkable works by Hert and Lumelsky in this field of study. In [10, 31], to achieve tangle-free planning, robots are prioritized and scheduled to move sequentially in a common planar and spatial environment that is free of obstacles. However, the sequential motion of a group of robots is not efficient and the planning may fall in deadlock under certain circumstances. Although simultaneous robot motion is mentioned in their later work on planar workspaces [11], it is not leveraged to solve deadlocks. Another

work by Sinden provides an algorithm for scheduling multiple robots moving simultaneously while avoiding tether tangling, but only under some special cases [32].

### 2.3. Summary

In this work, we consider the robot navigation problem for multiple tethered planar mobile robots. We aim at examining the realizability of a target cable configuration by different modes of robot motion, and developing path planning algorithms for the robots to achieve the given target cable configuration by Straight/Concurrent motion.

## 3. Background: non-intersecting target cable configurations and realizability

### 3.1. Problem formulation

Consider  $n$  point robots on a planar workspace  $\mathcal{W}$ . Each robot  $r_i, i = 1, \dots, n$ , must navigate from its starting position  $S_i$  to its target position  $T_i$ , while being attached to  $S_i$  by a flexible cable. The cables are assumed to remain on the ground and to be taut at all times; they can bend around other robots, and be pushed by other robots.

**Definition 1** (Cable line, cable configuration). *Because of the assumption that the cables are taut and can only bend around point robots, the cable of any robot at any time instant is a polygonal chain, which we call the robot's cable line. The final (target) cable line of a robot is the (desired) state of the robot's cable line after all robots have reached their target positions.*

A cable configuration consists of the cable lines of all robots at a given time instant. A final (target) cable configuration is the (desired) cable configuration after all robots have reached their targets.

Cable polygon in the following definition was originally defined as *retraction polygon* in [10].

**Definition 2** (Cable polygon). *The cable polygon  $\Pi_i$  of a given robot  $r_i$  is formed by closing the robot's target cable line with the straight-line segment  $(S_i, T_i)$  joining the robot's starting and target positions.*

We now introduce two important assumptions.

**Assumption 1** (Starting positions and cable polygons). *The starting position  $S_i$  of a robot  $r_i$  does not belong to any cable polygon  $\Pi_j, j \neq i$ .*

Assumption 1 fully covers the hypotheses of previous works [10, 31], which assume that  $\mathcal{W}$  is a convex polygon and that all starting positions lay on the boundary of  $\mathcal{W}$ . The extension to more general cases with obstacles present in the environment is discussed in Appendix C.

**Assumption 2** (No self loop). *When a target cable line contains repeated waypoints, we say that it contains self loops (see Fig. 3(a)) We assume that there is no self loop in any target cable line.*

self loops are obviously redundant and there is always a better solution. An example is presented in Fig. 3: The target cable configuration in Fig. 3(a) is valid in the sense that no cable tangle happens, but it is highly inefficient and can be replaced with an alternative simple cable layout as shown in Fig. 3(b).

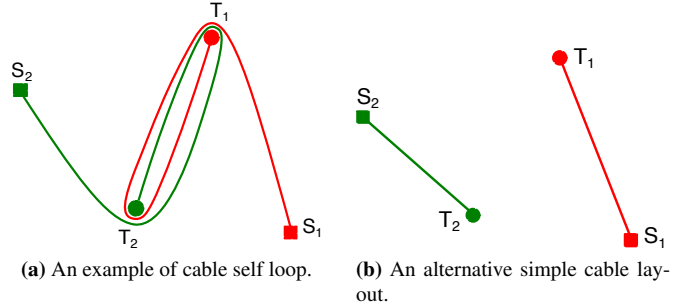


Fig. 3. An example of cable self loop and its alternative simple layout.

### 3.2. Non-intersecting target cable configurations

We say that a cable configuration is *non intersecting* if no pair of cable lines in that configuration intersect each other. In [8], the problem of finding non-intersecting target cable configurations is formulated as a graph problem.  $G = \{V, E\}$  contains all starting points  $\{S_1, \dots, S_n\}$  and target points  $\{T_1, \dots, T_n\}$  in its node set  $V$ , and all edges in the form of  $(S_i, T_j)$  in its edge set  $E$ . Finding non-intersecting target cable configuration is now equivalent to finding a set of consecutive edges from  $S_i$  to  $T_i$  for each robot  $r_i$  while observing cable property. An algorithm using exhaustive search method with pruning is suggested to identify and eliminate every route intersection case, producing all possible non-intersecting cable configurations. Regarding the cable intersection detection algorithm, readers may refer to [8] for more details. Note however that the algorithm would fail under certain circumstances. We discuss the failure cases and provide corrections in Appendix B.

### 3.3. Realizability of non-intersecting target cable configurations

We now study the realizability of a given non-intersecting target cable configuration (in the following text we shall omit the term “non-intersecting” when there is no possible confusion).

There are four reasonable modes of motion: Bent/Sequential, Bent/Concurrent, Straight/Sequential and Straight/Concurrent. Straight and Bent refer to the route that the robots have to follow during the navigation: Straight denotes that the robots moves in straight lines from their starting positions directly towards target positions, while Bent indicates that the robots follow their target cable lines. Meanwhile, Sequential and Concurrent refer to the schedule of the robot motion: Sequential indicates that the robots are prioritized and they have to move towards their target positions one at a time, while Concurrent denotes that the robots move to target positions simultaneously. The solution spaces of these different modes of

motion is shown in Fig. 4, and a thorough analysis is presented in the following sections.

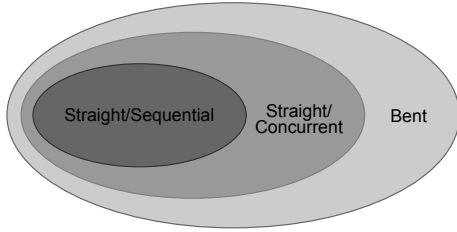


Fig. 4. Solution spaces of the different modes of motion (Bent, Straight/Concurrent, Straight/Sequential).

### 3.3.1. Realizability by Bent/Sequential

It is proved in [10] that: “If each robot moves along its target cable line, the final cable configuration will be the same as the target cable configuration.” Note that the proof is non-trivial because of the assumption that the cables remain taut at all time. A robot’s cable line will thus deform and auto-retract to maintain tautness if the robots that cause bends in its target cable line are not yet in position.

### 3.3.2. Realizability by Bent/Concurrent

It is straightforward to infer that Bent/Sequential could be regarded as an extreme case of Bent/Concurrent. Since Bent/Sequential mode of motion is proved to be able to achieve any feasible target cable configuration, it follows that Bent/Concurrent can produce a solution for any feasible target cable configuration as well.

The most efficient motion for this mode would be “just move”, which means that the robots move along their target cable lines at the same time. When robot  $r_i$  passes point  $T_j$  on its target cable line, if  $T_j$  has already been occupied by robot  $r_j$ , cable  $C_i$  wraps  $r_j$  from the desired direction; if  $r_j$  has not reached  $T_j$  yet,  $C_i$  will be retracted and will be pushed by  $r_j$  later from the correct side (see Fig. 5).

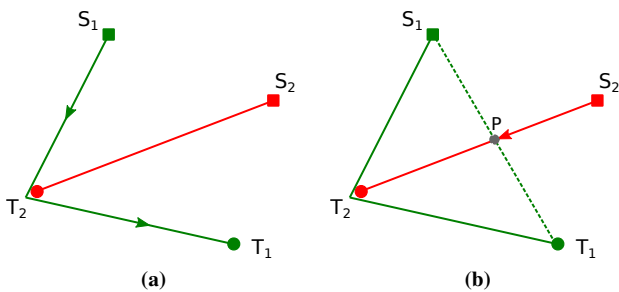


Fig. 5. An illustration of realizability by Bent/Concurrent. When  $r_1$  passes  $T_2$ : (a)  $r_2$  has reached  $T_2$ .  $C_1$  wraps around  $r_2$  at  $T_2$ ; (b)  $r_2$  has not reached  $T_2$  yet.  $C_1$  retracts to the dotted line and is pushed by  $r_2$  at  $P$  during  $r_2$ ’s navigation later.

Compared to Bent/Sequential motion, Bent/Concurrent requires less execution time as robots

do not need to wait and move one by one. However, restricting the robots to move along their target cable lines is still a waste of time and energy. The most efficient motion scheme would be straight-line motion for robots to navigate from starting to target positions.

### 3.3.3. Realizability by Straight/Sequential

In [10], Hert and Lumelsky provide an algorithm where robots are prioritized and scheduled to move sequentially in a straight line as much as possible. In this case, “each robot must move before any robot its cable line bends around has moved” [10]. With this observation, a directed graph can be constructed: each vertex in the graph represents a robot, and a directed edge from  $v_i$  to  $v_j$  implies that robot  $r_i$  must move before  $r_j$ . The order of robot motions can then be determined by extracting at each step the root node of the graph, which corresponds to the robot that does not have to wait for any other robots. In the event of loop occurrence in the graph, the robot motion falls in deadlock situation. As an illustration, Fig. 6 is the directed graph constructed from Fig. 1. Since cable  $C_1$ ,  $C_2$  and  $C_3$  have to wrap around robot  $r_2$ ,  $r_3$  and  $r_1$  at their target positions respectively, a loop is formed in the directed graph, and no root node can be extracted in this case. Therefore, there is no feasible solution for the target cable configuration by Straight/Sequential motion, leading to a deadlock situation.

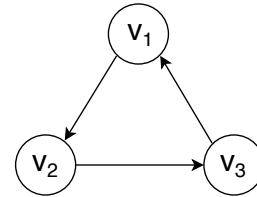


Fig. 6. The corresponding directed graph [10] for the target cable configuration in Fig. 1. A directed loop implies that it is a deadlock situation for Straight/Sequential motion.

This approach is intuitive, but it fails to detect all possible deadlocks. Consider the scenario depicted in Fig. 7(a), which is a deadlock situation for Straight/Sequential motion. However, with its corresponding directed graph as shown in Fig. 7(c), the robots’ motion order is extracted, and eventually leads to a wrong final cable configuration as shown in Fig. 7(b) [10].

A later work by Hert and Lumelsky [11] supplements the previous algorithm. In addition to the previous rule, they consider each pair of robots  $r_i$  and  $r_j$  that satisfies the following constraints:

1. there is no directed edge between  $v_i$  and  $v_j$  in the directed graph;
2. the straight-line paths of  $r_i$  and  $r_j$  cross each other.

Then an edge from  $v_i$  to  $v_j$  is added to the graph if  $T_j$  is in the cable polygon of  $r_i$ , and vice versa. This supplemented constraint plays an important role in deadlock detection. Recall

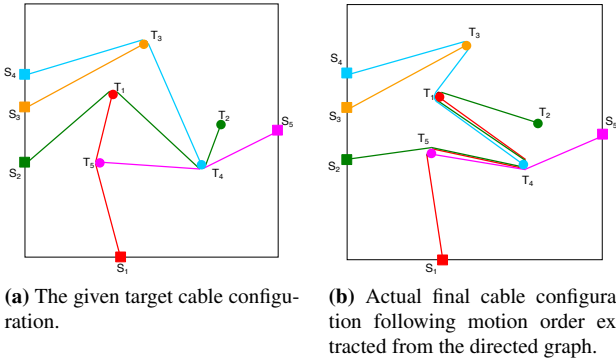


Fig. 7. An example of deadlock detection failure for Straight/Sequential motion with the algorithm proposed in [10].

the target cable configuration in Fig. 7(a). With this supplemented constraint, an edge from  $v_4$  to  $v_1$  should be added to Fig. 7(c), forming a directed loop  $v_1 - v_5 - v_4 - v_1$ , which reveals the deadlock nature of the target cable configuration by Straight/Sequential motion. However, this algorithm is still not complete in detecting all possible deadlock situations. It fails to include the case when straight-line paths of robots do not cross each other, but their target points are in each other's cable polygon. This case is a deadlock situation for Straight mode, and is illustrated in Fig. 9(e, f). We define it as *pair deadlock*, and detail the conception in Section 4.2.

### 3.3.4. Realizability by Straight/Concurrent

Straight/Sequential motion improves the efficiency compared to the Bent modes due to its shorter paths, yet it is a waste of time if the target cable configuration can be achieved by concurrent robot motion.

It is not difficult to infer that the solution space of Straight/Concurrent mode covers that of Straight/Sequential mode. In other words, target cable configurations that can be achieved by Straight/Sequential motion can also be achieved by Straight/Concurrent motion, with a more efficient solution; deadlock conditions for Straight/Concurrent motion must also be deadlock conditions for Straight/Sequential motion.

Although in [11], the simultaneous motion of robots is discussed, it is not leveraged to solve deadlocks. Take Fig. 7(a) as an example. As an output from their algorithm, the target cable configuration is a deadlock situation, and the path for  $r_4$  is  $S_4 - T_1 - T_4$ . However, this target cable configuration is shown to be realizable by Straight/Concurrent motion with the algorithms we present in the next section.

### 3.3.5. Summary

In this paper, we propose algorithms that (a) detect whether a given target cable configuration can be achieved by Straight/Concurrent motion, and (b) return a valid coordinated motion plan, if applies. When there is no feasible solution, some robots will be selected to move along their target cable lines to maintain the correctness of the final cable configuration.

## 4. Algorithm for Straight/Concurrent motion

### 4.1. Overview of the algorithm

The flow of the algorithm is as follows (see Fig. 8): given an input target cable configuration,

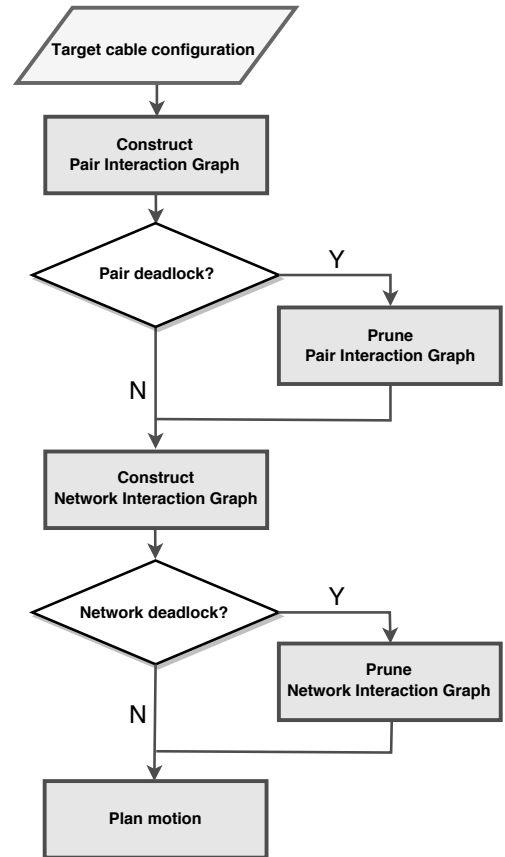


Fig. 8. Flow of the algorithm.

1. construct the Pair Interaction Graph (PIG), which encodes the interactions between pair of robots based on their cable polygons;
2. detect *pair deadlocks* in the PIG, and solve them (prune the PIG) by assigning one robot of each pair deadlock to follow its target cable line;
3. from the pruned PIG, construct the Network Interaction Graph (NIG), which encodes the network interactions induced by the pair interactions, taking into account the intersections of robot paths;

4. detect *network deadlocks* in the NIG, and solve them (prune the NIG) by assigning one robot involved in each network deadlock to follow its cable line;
5. from the pruned NIG, compute the final motion schedule.

The different steps of the algorithm are detailed in the following sections.

#### 4.2. Constructing the Pair Interaction Graph (PIG)

We consider first the elementary interactions that occur between a pair of robots. Those interactions are determined by the position of one robot's target with respect to the other robot's cable polygon (recall from Assumption 1 that a robot's starting position is always outside other robots' cable polygons). Given a pair of robots  $(r_i, r_j)$ , there are thus four types of pair interactions: (1)  $T_i \notin \Pi_j, T_j \notin \Pi_i$  [Fig. 9(a)]; (2)  $T_i \in \Pi_j, T_j \notin \Pi_i$  [Fig. 9(c)]; (3)  $T_i \notin \Pi_j, T_j \in \Pi_i$ ; (4)  $T_i \in \Pi_j, T_j \in \Pi_i$  [Fig. 9(e)]. Note that types 2 and 3 are symmetrical and will be treated together.

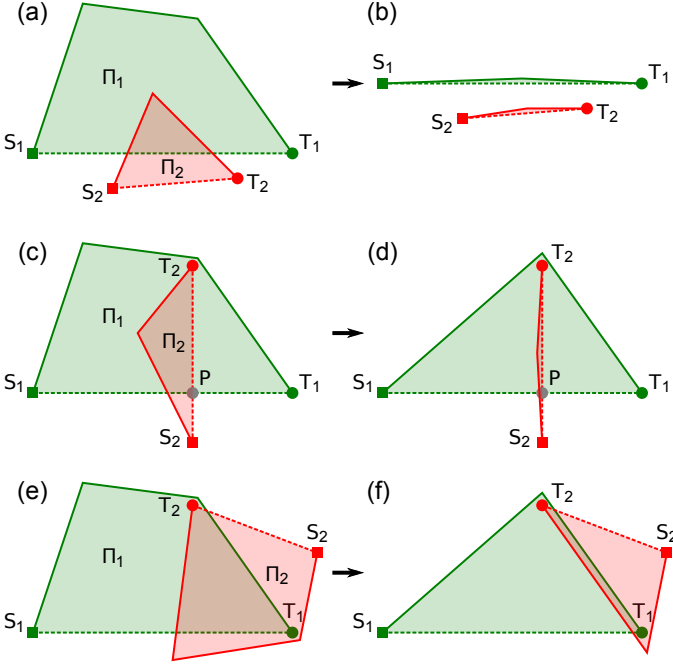


**Fig. 9.** Pair robot interactions are determined by the position of targets with respect to cable polygons. Left (a, c, e): cable polygons for type (1), (2-3), and (4) respectively. Right (b, d, f): retracted cable polygons after removing robots that are not involved in the pair interaction.

Since we are interested in pair interactions, we suppose that the other robots are temporarily removed from the problem (multi-robot interactions will be addressed in Section 4.4). As a result, the cable polygons are *retracted* as in Fig. 9(b, d, f). Note that the retraction process does not affect the interaction types just described.

The following propositions establish the motion priorities induced by each type of pair interactions.

**Proposition 1.** *If  $T_i \notin \Pi_j$  and  $T_j \notin \Pi_i$ , then there are no priority induced by the pair interaction.*

*Proof.* We prove in Appendix A that, in this case, the two segments  $(S_i, T_i)$  and  $(S_j, T_j)$  do not intersect. Thus, the retracted cable polygons are reduced to two independent segments [Fig. 9(b)], inducing no motion priority between  $r_i$  and  $r_j$ .  $\square$

**Proposition 2.** *If  $T_i \in \Pi_j$  and  $T_j \notin \Pi_i$ , then, with  $P$  denoting the intersection point between  $(S_i, T_i)$  and  $(S_j, T_j)$ ,  $r_j$  must pass  $P$  before  $r_i$  does.*

*Proof.* We prove in Appendix A that, in this case, the two segments  $(S_i, T_i)$  and  $(S_j, T_j)$  must intersect, at a point  $P$ . One can then see that  $r_i$  must pass  $P$  before  $r_j$  does. Fig. 9(d) illustrates this statement: the motion paths  $(S_1, T_1)$  and  $(S_2, T_2)$  intersect at  $P$  and  $T_2 \in \Pi_1$ . Clearly,  $r_1$  must pass  $P$  before  $r_2$  does, so that  $r_2$  can “push” the cable line of  $r_1$ .  $\square$

**Proposition 3.** *If  $T_i \in \Pi_j$  and  $T_j \in \Pi_i$ , then there is a deadlock, which we call a pair deadlock. One of the two robots must diverge from the straight line motion.*

*Proof.* We prove in Appendix A that, in this case, the two segments  $(S_i, T_i)$  and  $(S_j, T_j)$  do not intersect. This case implies a deadlock situation, which we call *pair deadlock*, as illustrated in Fig. 9(f). The motion paths  $(S_1, T_1)$  and  $(S_2, T_2)$  do not intersect, but  $T_1 \in \Pi_2$  and  $T_2 \in \Pi_1$ . When  $r_1$  and  $r_2$  move along their motion paths, the final cable configuration will be two independent segments  $(S_1, T_1)$  and  $(S_2, T_2)$ , which are different from their retracted polygons as shown in Fig. 9(f). In this case,  $r_1$  ( $r_2$ ) has to diverge from the straight line motion and move around  $T_2$  ( $T_1$ ) in order to push  $C_2$  ( $C_1$ ) to the desired target cable configuration.  $\square$

Based on the above propositions, we can formulate Algorithm 1 to encode pair interactions. The algorithm constructs a directed graph, termed the Pair Interaction Graph (PIG), whose vertices represent the robots, and whose edges encode motion priority relationships: (1) if there is a unidirectional edge pointing from vertex  $v_i$  to vertex  $v_j$ , then robot  $r_i$  must pass the intersection point before  $r_j$ ; (2) if there is a bidirectional edge between vertex  $v_i$  and vertex  $v_j$ , then there is a pair deadlock.

#### 4.3. Detecting and solving pair deadlocks

When a pair deadlock occurs, one of the two robots must diverge from the straight line motion. Consider the deadlock case of Fig. 9(f): the deadlock can be solved by (i) one robot, say  $r_1$ , moves in a straight line from  $S_1$  to  $T_1$ ; (ii) the other robot,  $r_2$ , follows its target cable line (start from  $S_2$ , wrap around  $T_1$ , then go to  $T_2$ ). Although motion paths other than the robot target cable line are possible in stage (ii), we shall not consider them to avoid too much complexity.

Accordingly, we propose the following steps to address pair deadlocks:

1. Detect all pair deadlocks (by finding all bi-directional edges in the PIG), and put the robots involved in those deadlocks into a list  $\bar{L}$ ;

---

**Algorithm 1** Constructing the Pair Interaction Graph
 

---

**Input:** Target cable configuration

**Output:** Pair Interaction Graph (PIG)

```

1: for  $i = 1 : n$  do
2:   Add a vertex  $v_i$  for each robot  $r_i$ 
3: end for
4: for  $i = 1 : n - 1$  do
5:   for  $j = i + 1 : n$  do
6:     if  $(S_i, T_i)$  and  $(S_j, T_j)$  intersect at  $P$  then
7:       if  $T_i \in \Pi_j$  then
8:         Add an edge from  $v_j$  to  $v_i$ , labeled  $\{v_j \xrightarrow{P} v_i\}$ 
9:       else
10:        Add an edge from  $v_i$  to  $v_j$ , labeled  $\{v_i \xrightarrow{P} v_j\}$ 
11:      end if
12:     else if  $T_i \in \Pi_j$  and  $T_j \in \Pi_i$  then
13:       Add a bi-directed edge between  $v_i$  and  $v_j$ 
14:     end if
15:   end for
16: end for

```

---

- Iteratively extract one robot, say  $r_i$ , from  $\tilde{L}$ ; put it in a list  $L^*$ ; remove  $r_i$  completely from the problem; update accordingly the PIG and  $\tilde{L}$ ; repeat until  $\tilde{L}$  is empty.

At the end of this algorithm, one has a list  $L^*$  of robots that will be forced to follow their target cable lines after all other robots have moved, and a PIG that no longer contains pair deadlocks (pruned PIG).

In step 2, there are diverse methods to choose which robot to remove first from the problem. One can for instance choose the robot that is involved in the largest number of pair deadlocks, or the one whose target cable line generates the largest detour as compared to the straight line.

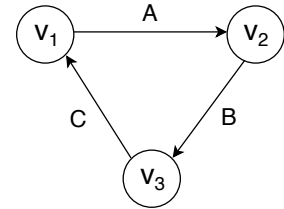
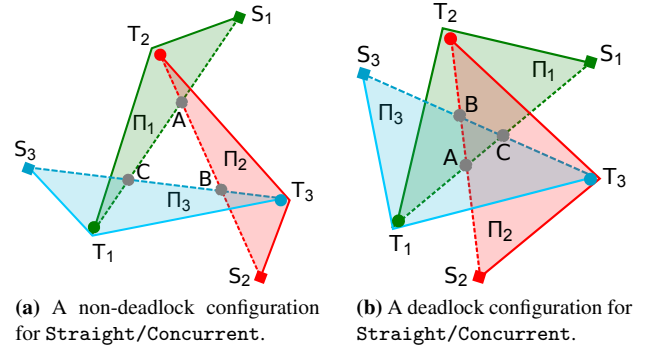
#### 4.4. Constructing the Network Interaction Graph (NIG)

We have seen in Section 4.2 that pair interactions of type 1 do not induce priority, while pair interactions of type 4 induce deadlock situations, which are subsequently solved by forcing one of the robots of the pairs to follow its target cable line. As also discussed, pair interactions of types 2 and 3 give rise to priority relationships between the two robots of the pair at their intersection point. These relationships can in turn lead to *network* interactions if some robots are simultaneously involved in more than one pair interactions.

To illustrate, consider the scenario depicted in Fig. 10(a). The pair interactions give rise to the PIG of Fig. 10(c), which includes a circular priority chain. Yet, this situation is not deadlocked, since the following coordinated motion leads to the correct target cable configuration:  $r_1$ ,  $r_2$  and  $r_3$  move along their  $(S_i, T_i)$  motion paths at the same velocity. By doing so, they will indeed pass respectively points  $A$ ,  $B$  and  $C$  at the same time, which in turn satisfies the requirement that  $r_1$  passes  $A$  before  $r_2$  does,  $r_2$  passes  $B$  before  $r_3$  does, and  $r_3$  passes  $C$  before  $r_1$  does.

Consider now the scenario depicted in Fig. 10(b). The pair interactions give rise to the same PIG of Fig. 10(c). However,

one can see that the situation is deadlocked. The intersection points between each pair of robots have different relative positions along robots'  $(S_i, T_i)$  motion paths now:  $C$  is closer to  $S_1$  than  $A$ ,  $A$  is closer to  $S_2$  than  $B$ , and  $B$  is closer to  $S_3$  than  $C$ . Indeed, the constraint imposed by the three directed edges in PIG (see Fig. 10(c)) implies that  $r_1$  passes  $C$  before  $r_2$  passes  $A$ ,  $r_2$  passes  $A$  before  $r_3$  passes  $B$ , and  $r_3$  passes  $B$  before  $r_1$  passes  $C$ . It is thus clear that the situation is deadlocked.



(c) Pair interaction graph (same for both configurations).

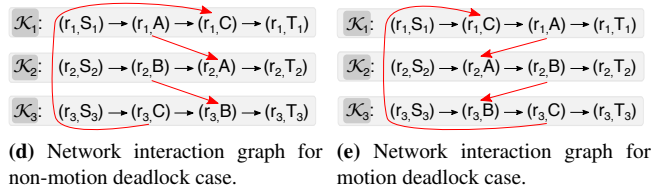


**Fig. 10.** Network interactions are determined, not only by the priority relationship between the robots at their intersection point, but also by the relative arrangement of the intersection points.

It appears from the two scenarios discussed above that correctly handling network interactions requires taking into account, not only the priority relationship between the robots at their intersection points, but also the *relative arrangement of those intersection points*. To encode this information, we propose to construct the Network Interaction Graph (NIG) whose vertices are the *events* “robot  $r_i$  passes intersection point  $P$ ”, denoted  $(r_i, P)$ , and whose directed edges encode the temporal relationships among the events, as follows [see Fig. 10(d, e) for illustrations]:

- For each robot  $r_i$  of the PIG, add to the NIG a chain  $\mathcal{K}_i$ :  $(r_i, S_i) \rightarrow (r_i, P_1) \rightarrow \dots \rightarrow (r_i, P_m) \rightarrow (r_i, T_i)$ , where  $P_1, \dots, P_m$  are the ordered intersection points along the segment  $(S_i, T_i)$ ;

2. For each edge  $\{v_i \xrightarrow{P} v_j\}$  of the PIG, add to the NIG a directed edge from  $(r_i, P)$  (in  $\mathcal{K}_i$ ) to  $(r_j, P)$  (in  $\mathcal{K}_j$ ).

#### 4.5. Detecting and solving network deadlocks

We can now state and prove the following proposition.

**Proposition 4.** *If the NIG contains a directed cycle, then there exists a network deadlock.*

*Proof.* Note that an edge  $(r_i, P) \rightarrow (r_i, P')$  added in step 1 of the algorithm to construct the NIG (intra-chain edge) encodes the requirement that robot  $r_i$  must pass point  $P$  before point  $P'$ . We note this relationship  $(r_i, P) < (r_i, P')$ .

An edge  $(r_i, P) \rightarrow (r_j, P)$  added in step 2 (inter-chain edge) encodes the requirement that robot  $r_i$  must pass point  $P$  before robot  $r_j$  passes  $P$ . We note this relationship  $(r_i, P) < (r_j, P)$ .

Observe that the relationship “ $<$ ” just defined, by its temporal nature, is a strict order relationship in the set of events, i.e. it verifies the irreflexivity, antisymmetry, and transitivity properties.

Consider now a directed cycle in the NIG. Such a cycle induces a cycle for the strict order relationship “ $<$ ”, which is clearly not satisfiable. Therefore, there exists at least one priority requirement that cannot be satisfied in the cycle, i.e. a deadlock situation.  $\square$

When there is a network deadlock, one of the involved robots has to diverge from the straight-line motion, similarly to the pair deadlock case. Accordingly, we propose the following steps to address network deadlocks:

1. Detect all network deadlocks (by finding all directed cycles in the NIG), and put the robots involved in those deadlocks into a list  $\tilde{L}$ ;
2. Iteratively extract one robot, say  $r_i$ , from  $\tilde{L}$ ; put it in the list  $L^*$  (the same as used previously for solving pair deadlocks); remove  $r_i$  completely from the problem; update accordingly the NIG and  $\tilde{L}$ ; repeat until  $\tilde{L}$  is empty.

At the end of this algorithm, one has a list  $L^*$  of robots that will be forced to follow their target cable lines after all other robots have moved, and a NIG that no longer contains network deadlocks (pruned NIG).

Similarly to the case of pair deadlocks, there are diverse methods, in step 2, to choose which robot to remove first from the problem. One can for instance choose the robot that is involved in the largest number of network deadlocks, or the one whose target cable line generates the largest detour as compared to the straight line.

#### 4.6. Computing the final motion schedule

When we coordinate the motion of a pair of robots at the intersection point of their  $(S, T)$  motion paths, we could either make the lower priority robot wait until the higher priority robot passes the point, or adjust the speed of the robots to produce continuous motions. In this work, the waiting scheme is

adopted for illustration. A coordinated motion plan with shortest traveling time is generated if the target cable configuration can be achieved by Straight/Concurrent robot motion.

In the following procedures,  $(r_i, P^-)$  and  $(r_i, P^+)$  denote the predecessor and successor of  $(r_i, P)$  on the chain  $\mathcal{K}_i$  respectively.  $\mathcal{T}_i$  represents the time-line for robot  $r_i$ , and  $T_{i,P}$  is the time-stamp on  $\mathcal{T}_i$ , upon which robot  $r_i$  starts to navigate from  $(r_i, P)$  to  $(r_i, P^+)$ . Weight  $w_{i,P}$  of node  $(r_i, P)$  indicates the amount of time that  $r_i$  takes to travel from  $(r_i, P^-)$  to  $(r_i, P)$ .

From the NIG (which we suppose does not contain any cycle), we can extract a coordinated motion schedule for the robots to achieve the target cable configuration as follows:

1. For each chain  $\mathcal{K}_i$  of the NIG,  $i = 1, \dots, n$ , calculate and assign the weight to every node (weight is 0 for  $(r_i, S_i)$ );
2. Initialize time-line  $\mathcal{T}_i$  for each robot  $r_i$ ,  $i = 1, \dots, n$ ;
3. For the root node  $(r_i, R)$  in  $\mathcal{K}_i$ ,  $i = 1, \dots, n$ ,
  - (a). If there is no incoming inter-chain edge from any  $\mathcal{K}_j$ ,  $i \neq j$ , append traveling time  $w_{i,R}$  to  $\mathcal{T}_i$ , and remove  $(r_i, R)$  from the NIG;
  - (b). If there is an incoming inter-chain edge from an already removed node  $(r_j, P)$  in  $\mathcal{K}_j$ ,  $w_{i,R}$  must be appended to  $\mathcal{T}_i$  at a time-stamp that is *no earlier than*  $T_{j,P}^1$ , after which  $(r_i, R)$  and this incoming inter-chain edge are removed from the NIG;
4. Repeat step 3 until there is only the node  $T_i$  left in each chain  $\mathcal{K}_i$ ,  $i = 1, \dots, n$  of the NIG;
5. Make robots in  $L^*$  move along their target cable lines after all other robots have reached their target positions.

A detailed example is presented in Section 5.

#### 4.7. Complexity of the algorithms

We now analyze the complexity of the algorithms just presented as a function of the number  $n$  of robots. Note first that, for each robot  $r_i$ , the number of vertices (and edges) of its cable polygon  $\Pi_i$  is  $O(n)$  since it is bounded by the total number of robots (the cables can only wrap around other robots).

##### 4.7.1. Pair Interaction Graph

To construct the PIG, the step with the highest complexity is to check whether  $T_i \in \Pi_j$  for all pairs  $(i, j)$ . The test  $T_i \in \Pi_j$  has a linear complexity in the number of edges of  $\Pi_j$ , which is  $O(n)$ . Thus, the construction of the PIG has a complexity of  $O(n^3)$ .

Detecting pair deadlocks involves finding all bi-directional edges in the PIG and can therefore be done in  $O(n^2)$ .

There are potentially  $O(n)$  deadlocked robots. For a deadlocked robot, say robot  $r_i$ , one needs to remove it and update the PIG accordingly, which can be done in  $O(n^2)$ . Thus, pruning the PIG can be done in  $O(n^3)$ .

<sup>1</sup>Here we use a relaxed chronological order *no earlier than* for a directed inter-chain edge from  $(r_j, P)$  in  $\mathcal{K}_j$  to  $(r_i, R)$  in  $\mathcal{K}_i$  in order to exempt  $r_i$  from the unnecessary waiting time for the whole duration  $w_{i,P}$ .

#### 4.7.2. Network Interaction Graph

To construct the NIG, the main step is to compute, for each robot  $r_i$ , the intersections of  $(S_i, T_i)$  with all the  $(S_j, T_j)$  and order those intersections along  $(S_i, T_i)$ . This can be done in  $O(n^2 \log(n))$ .

Detecting network deadlocks involves checking whether the NIG has a cycle, which can be done in  $O(n^2)$  (topological sort). Pruning the NIG can be done in  $O(n^3)$ .

#### 4.7.3. Motion schedule

The algorithm for scheduling the robot motions is linear in the number of nodes of the NIG and is therefore  $O(n^2)$ .

From the above analysis, the worst time-complexity of the full pipeline is  $O(n^3)$ .

## 5. Examples

### 5.1. An example from Hert & Lumelsky 1996

In this section, we validate our proposed algorithms with the example previously shown in Fig. 7(a), which is a deadlock situation for Straight/Sequential motion. We show that the target cable configuration can be achieved by Straight/Concurrent motion and  $r_4$  does not need to take a detour as in the output of the algorithm in [11].

The intermediate stages of achieving the target cable configuration with our proposed algorithms are shown in Fig. 11. In addition, a step-wise illustration of motion scheduling is presented in Fig. 12.

To avoid the wrong final cable configuration as shown in Fig. 7(b),  $r_4$  must pass A before  $r_1$  does. It is not possible in Straight/Sequential motion, since  $r_1$  has to reach its target position before  $r_4$  does. However, moving in Straight/Concurrent motion following the local navigation priority as indicated in Fig. 11(d), which contains no directed cycle, the target cable configuration can be achieved successfully.

### 5.2. Hardware experiment

We validate the proposed algorithms in a hardware experiment. We consider the large-scale, multi-robot 3D Printing system previously developed by our group [3]. The tethers are indispensable here to deliver the fresh concrete from the mixer to the print nozzle. The size of each mobile robot is  $960 \times 793 \times 296$  mm. Each cable is 10 m in length and has a bend radius of 110 mm. We implemented the coordinated motion plan of Fig. 1.  $(S_i, T_i)$  segment for each robot was 7 m. The maximal velocity of each robots was 0.6 m/s. To achieve the target cable configuration, at each intersection point, the robots must follow the motion priority as indicated in the NIG (see Fig. 10(d)).

Fig. 13 shows snapshots of the coordinated motions when the robots respected the calculated motion priority. The mobile robots moved in Straight/Concurrent mode: they were commanded to move simultaneously along their  $(S_i, T_i)$  straight-line segments. It is worthy of mention that at 14 s in the video of the experiment,  $r_2$  stopped and waited until  $r_1$  passed

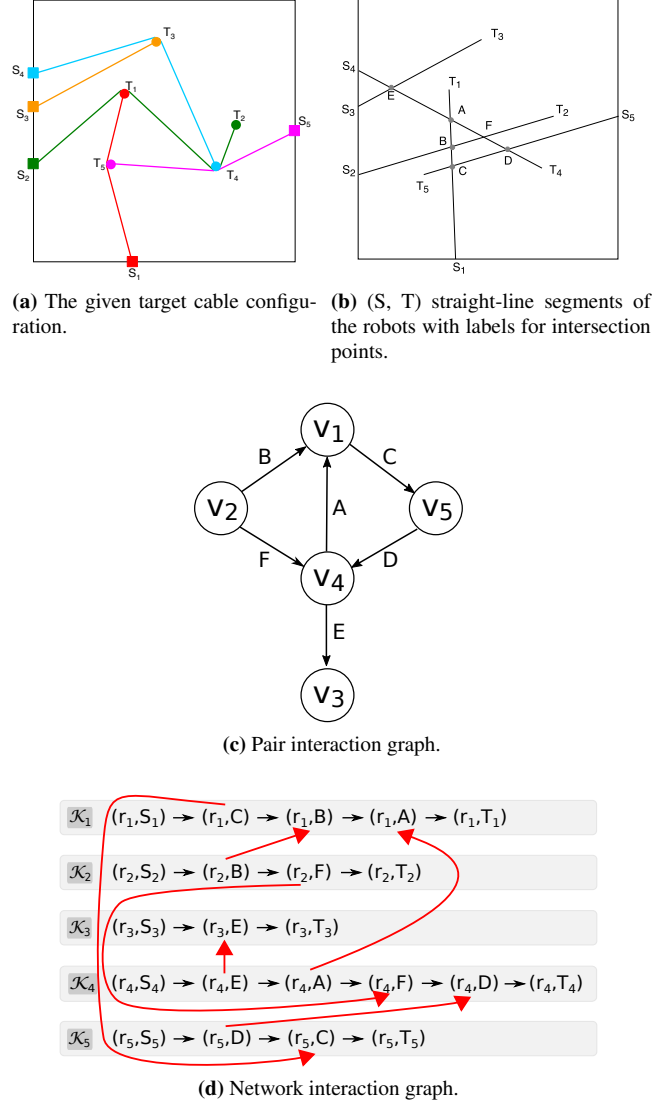
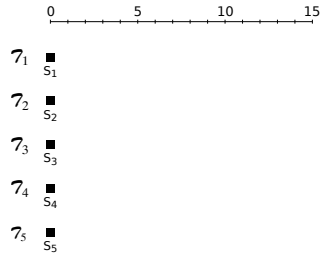
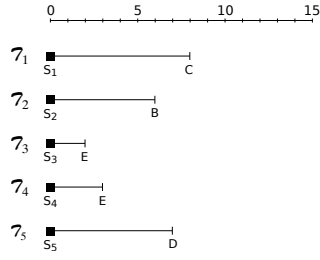


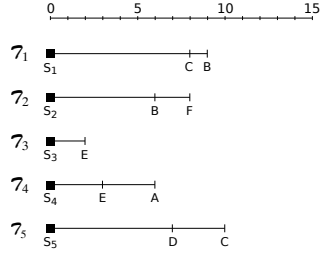
**Fig. 11.** The proposed algorithms are validated with a deadlocked target cable configuration for Straight/Sequential motion.



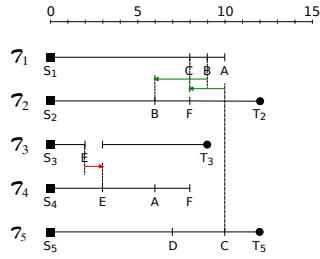
(a) Initialized time-lines for the robots.



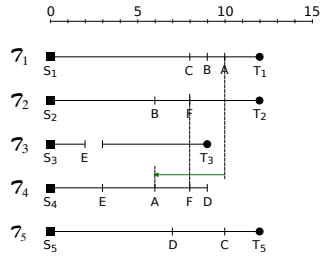
(c) Schedule step 1.



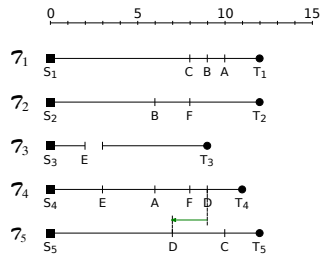
(e) Schedule step 2.



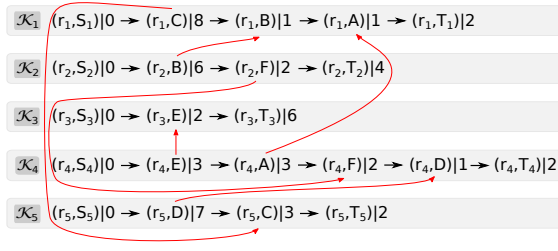
(g) Schedule step 3.



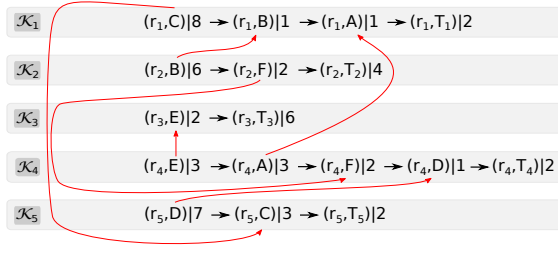
(i) Schedule step 4.



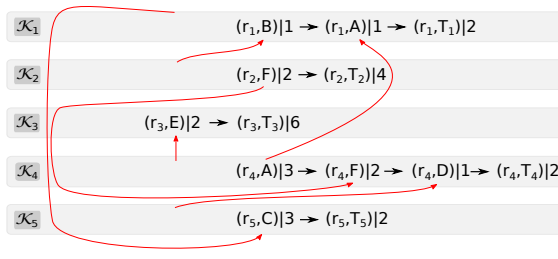
(k) Schedule step 5.



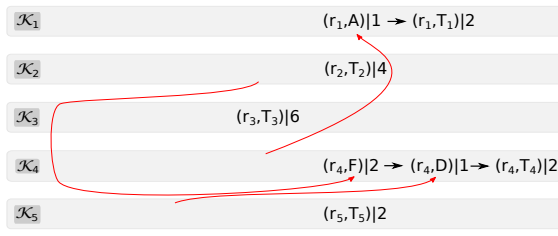
(b) The weighted NIG.



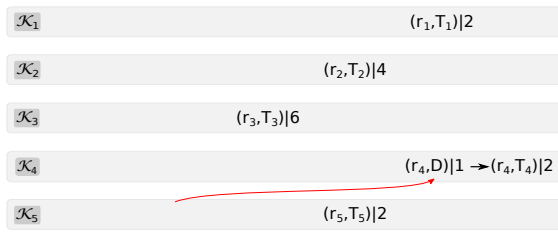
(d) Updated NIG after step 1.



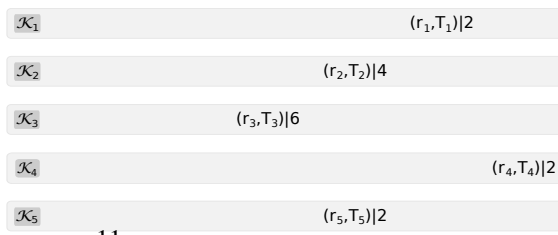
(f) Updated NIG after step 2.



(h) Updated NIG after step 3.



(j) Updated NIG after step 4.



(l) Updated NIG after step 5.

Fig. 12. Motion schedule generation for target cable configuration in Fig. 7(a)

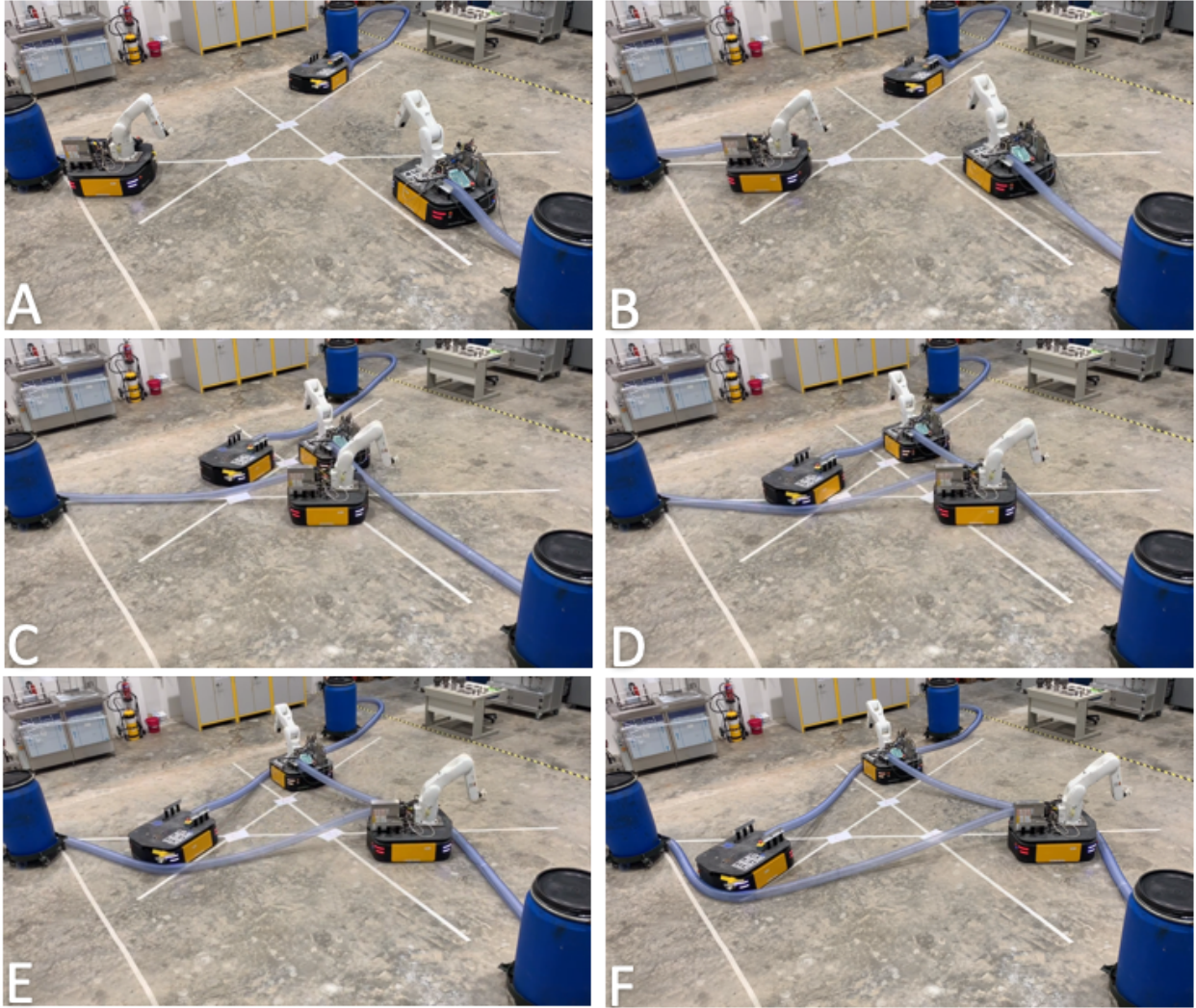


**Fig. 13.** Snapshots of the coordinated motions that achieve the desired target cable configuration. See the full video of the experiment at <https://youtu.be/Wdk9E0bB4yA>. A. Tethered robots at starting positions; B. Navigating towards target locations in concurrent straight-line motion; C. Passing intersection points with calculated priority; D. Pushing other robot's cable during navigation; E. Navigation in progress; F. Achieving final (target) cable configuration.

point  $A$ , after which  $r_2$  passed  $A$  and proceeded towards  $T_2$ . This movement reflects the motion priority of  $r_1$  and  $r_2$  at point  $A$ :  $r_1$  must pass  $A$  before  $r_2$  does. Although the robots were not strictly points, and that the tethers were not perfectly flexible, the target cable configuration could be achieved as the robot motions respected the calculated priorities at the intersection points. The result was evaluated purely based on positions of the robots, without taking their orientations into account.

By contrast, Fig. 14 shows snapshots of a second run, where the robots did not respect the calculated priorities at the intersection points. For better illustration of motion order at each intersection point, the robots were commanded to move in Straight/Sequential mode in the order of  $r_1$ ,  $r_2$  and  $r_3$  (see Fig. 2(b)). Therefore,  $r_1$  already reached  $T_1$  before  $r_3$  started to move (see Fig. 14D), which violated the motion priority at point  $C$ :  $r_3$  must pass  $C$  before  $r_1$  does. When  $r_3$  navigated towards  $T_3$ , it had to push  $C_1$  from  $C$  all the way to  $T_3$ , resulting in a wrong final cable configuration as shown in Fig. 14F. Due

to the limitation in tether length and the elastic property of the tethers,  $r_1$  was dragged back when  $C_1$  was pushed forward by  $r_3$ , and  $r_3$  failed to reach its target position.

A comparison of the total travel distance and the travel time for the above mentioned two hardware implementations is provided in Table 1. Data for Bent/Concurrent and Bent/Sequential modes was also computed for systematical comparison.

Table 1: Comparison of travel distance and travel time for different motion modes.

Motion mode	Straight/ Concurrent	Straight/ Sequential	Bent/ Concurrent <sup>2</sup>	Bent/ Sequential <sup>2</sup>
Total travel distance (m)	21	21	30	30
Travel time (s)	14	40	20	60

<sup>2</sup>Note that Bent/Concurrent and Bent/Sequential modes were not implemented in hardware experiment. The data was computed based on the robot velocity and tether length.

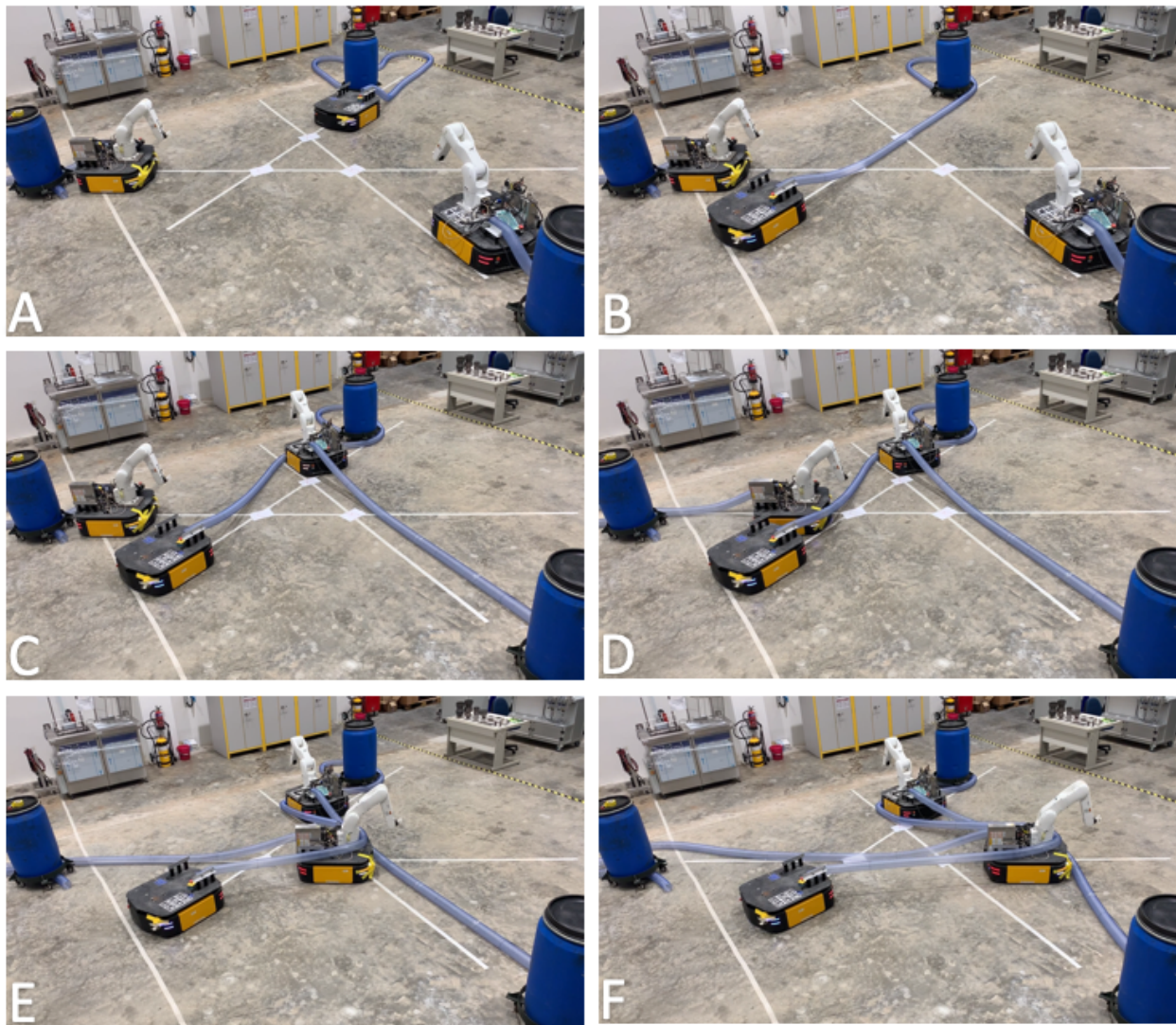


**Fig. 14.** Snapshots of the motions that fail to achieve the desired target cable configuration. See second part of the video <https://youtu.be/Wdk9E0bB4yA>. A. Tethered robots at starting positions; B. Robot  $r_1$  passing A before  $r_2$  as calculated; C. Robot  $r_2$  passing B before  $r_3$  as calculated; D. Robot  $r_3$  pushing  $r_1$ 's cable from the wrong side as the motion order of  $r_1$  and  $r_3$  at C is wrong; E. Robot  $r_3$  continuing its navigation; F. Resulting in wrong final cable configuration.

## 6. Conclusion

We have considered the motion planning problem for multiple tethered planar (point) mobile robots. We have presented motion planning algorithms for the robots to achieve a given target cable configuration by straight-line and concurrent (Straight/Concurrent) motions. The algorithms (i) identify whether the target cable configuration was deadlocked; (ii) return a valid coordinated motion plan accordingly. The correctness of the algorithms was proved in the process of algorithm development, and the worst time-complexity of the full pipeline was shown to be  $O(n^3)$ .

The proposed algorithms have been validated in both simulations and hardware experiments: we showed that, using our algorithms, the tethered robots could achieve a target cable configuration that involved a deadlock situation for Straight/Sequential motions, and that could not be solved by algorithms previously proposed in the literature.

During the hardware implementation, we found that for some applications, it could be challenging to design a tether management mechanism to keep the tether taut and retractable. In addition, robot size and geometry need to be taken into account during motion planning, especially for the purpose of collision avoidance. Our future work will consider integrating tether stiffness property and robot model into the proposed algorithms.

## Acknowledgment

This work was partially supported by the Medium-Sized Centre funding scheme (awarded by the National Research Foundation, Prime Minister's Office, Singapore) and by Sembcorp Design & Construction Pte Ltd. The authors would like to thank Hung Pham, Teguh Santoso Lembono and Lim Jian Hui for their constructive remarks on earlier versions of the manuscript, Lim Jian Hui and Panda Biranchi for their helps with the experiment.

## Appendix

### Appendix A. Proofs of the pair interaction propositions

We first need a topological lemma, which is also used in Jordan's proof of the Jordan curve theorem (see Lemma 1 of [33]).

**Lemma 1.** *Consider a polygon  $\Pi$ , a point  $S$  in the exterior of  $\Pi$ , and a continuous path starting from  $S$  and ending at  $T$ . Then  $T$  is in the interior of  $\Pi$  if and only if  $\mathcal{P}$  intersects the boundary of  $\Pi$  an odd number of times.*

We can now prove the following propositions, which are required by the pair interaction propositions of Section 4.2.

**Proposition 5.** *Assume that  $S_i, T_i \notin \Pi_j$  and  $S_j, T_j \notin \Pi_i$ , then the two segments  $(S_i, T_i)$  and  $(S_j, T_j)$  do not intersect.*

*Proof.* Assume by contradiction that  $(S_i, T_i)$  and  $(S_j, T_j)$  intersect at a point  $P$ . Consider the cable line  $C_j$  of robot  $r_j$ . By lemma 1,  $C_j$  will intersect the boundary of  $\Pi_i$  an even number of times. Since  $C_j$  has zero intersection with  $C_i$  (cable lines are non intersecting),  $C_j$  must intersect  $(S_i, T_i)$  an even number of times. Since  $(S_i, T_i)$  already intersects  $(S_j, T_j)$  at one point  $P$ , the total number of intersections between  $(S_i, T_i)$  and the boundary of  $\Pi_j$  is odd. By lemma 1, either  $S_i$  or  $T_i$  must therefore be in the interior of  $\Pi_j$ , which raises a contradiction.  $\square$

**Proposition 6.** *Assume that  $S_i \notin \Pi_j, S_j \notin \Pi_i, T_i \in \Pi_j, T_j \notin \Pi_i$ , then the two segments  $(S_i, T_i)$  and  $(S_j, T_j)$  must intersect.*

*Proof.* Assume by contradiction that  $(S_i, T_i)$  and  $(S_j, T_j)$  do not intersect. By lemma 1,  $C_i$  will intersect boundary of  $\Pi_j$  for odd number of times. Since  $C_i$  does not intersect  $C_j$  under the problem formulation,  $C_i$  must intersect  $(S_j, T_j)$  for odd number of times. The assumption that  $(S_j, T_j)$  and  $(S_i, T_i)$  do not intersect then implies that  $(S_j, T_j)$  intersects  $\Pi_i$  for odd number of times. Therefore either  $S_j$  or  $T_j$  has to be in the interior of  $\Pi_i$ , which raises a contradiction.  $\square$

**Proposition 7.** *Assume that  $S_i \notin \Pi_j, S_j \notin \Pi_i, T_i \in \Pi_j, T_j \in \Pi_i$ , then the two segments  $(S_i, T_i)$  and  $(S_j, T_j)$  do not intersect.*

*Proof.* Assume by contradiction that  $(S_i, T_i)$  and  $(S_j, T_j)$  intersect at a point  $P$ . By lemma 1,  $(S_i, T_i)$  will intersect boundary of  $\Pi_j$  for odd number of times, and  $C_j$  will intersect boundary of  $\Pi_i$  for odd number of times. Since  $(S_i, T_i)$  and  $(S_j, T_j)$  intersect at  $P$ ,  $(S_i, T_i)$  will intersect  $C_j$  for even number of times. Therefore  $C_j$  will intersect  $C_i$  for odd number of times, which raises a contradiction as cable lines are non intersecting.  $\square$

## Appendix B. Revising and supplementing Hert and Lumelsky 1997

In this section, route intersection detection algorithms for case 1(b) and 2(b) of the paper [8] are supplemented and revised. Some background terms are first introduced here.

A *cable route* ( $\mathcal{R}$ ) for robot  $r_i$  through graph  $G$  is defined as the set of adjacent edges leading from  $S_i$  to some node. Without loss of generality, it is assumed that no three consecutive nodes from a single route are collinear. Therefore, any two adjacent edges in a route form two distinct angles, one convex ( $< \pi$ ) and the other concave ( $> \pi$ ).

To find a feasible target cable configuration from  $G$ , the most fundamental task is to identify whether there is any route intersection in a given cable configuration. As discussed in [8], there are five different ways  $\mathcal{R}_A$  and  $\mathcal{R}_B$  can meet at a node  $T_k$ , considering the relative placement of edges from  $\mathcal{R}_A$  and  $\mathcal{R}_B$ :

1.  $T_k$  is the last node of one of the routes, say  $\mathcal{R}_A$ .  $\mathcal{R}_A$  has one edge incident to  $T_k$  and  $\mathcal{R}_B$  has two. The routes meet in one of the following two ways:

- (a)  $\mathcal{R}_A$  and  $\mathcal{R}_B$  do not share an edge incident to  $T_k$ ;
- (b)  $\mathcal{R}_A$  and  $\mathcal{R}_B$  do share an edge incident to  $T_k$ .

2.  $T_k$  is not the last node of either of the routes. Each route has two edges incident to  $T_k$ . There are three cases as the following:

- (a)  $\mathcal{R}_A$  and  $\mathcal{R}_B$  share no edge incident to  $T_k$ ;
- (b)  $\mathcal{R}_A$  and  $\mathcal{R}_B$  share one edge incident to  $T_k$ ;
- (c)  $\mathcal{R}_A$  and  $\mathcal{R}_B$  share both edges incident to  $T_k$ .

Route intersection may occur in cases from 1(a) to 2(b), but can be avoided in case 2(c). Besides the above possible intersections, there is one more case where two routes do not intersect at certain node, instead, they intersect in their interiors. Readers may refer to [8] for more details on the cable intersection detection algorithm, but the algorithm for case 1(b) is not complete, and that for case 2(b) needs revision. In the following section, we provide the revised and supplemented algorithms.

#### Appendix B.1. Detecting Route Intersection (revised and supplemented)

##### Appendix B.1.1. Case 1(b)

**Case 1(b):** Suppose  $\mathcal{R}_A$  and  $\mathcal{R}_B$  have one or more edges in common, and one of them is the last edge for  $\mathcal{R}_A$ .  $T_l$  is the goal node of  $\mathcal{R}_A$ .

In [8], the authors conclude this case as the following:

Let  $e_{a1}$  and  $e_{b1}$  be the two edges from  $\mathcal{R}_A$  and  $\mathcal{R}_B$ , immediately before this common set of edges. Let  $e_{b2}$  be the edge from  $\mathcal{R}_B$  immediately after the common set of edges. Let  $e_{fc}$  be the first edge shared by  $\mathcal{R}_A$  and  $\mathcal{R}_B$ , and  $e_{lc}$  the last edge shared by  $\mathcal{R}_A$  and  $\mathcal{R}_B$ .

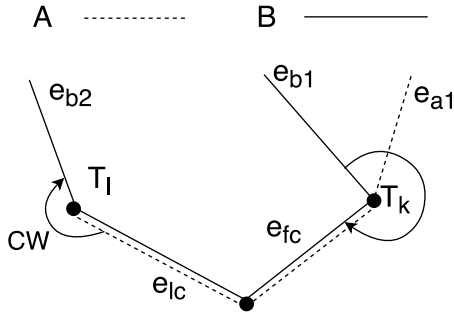


**Fig. B.15.** Case 1(b).  $\mathcal{R}_A$  and  $\mathcal{R}_B$  intersect at  $T_l$ . (The figure is taken from [8] Fig. 11.)

**Lemma 2**  $\mathcal{R}_A$  and  $\mathcal{R}_B$  intersect at  $T_l$  if and only if  $e_{a1}$  is contained in the clockwise (counterclockwise) angle from edge  $e_{b1}$  to  $e_{fc}$  and the clockwise (counterclockwise) angle from  $e_{lc}$  to  $e_{b2}$  is  $> \pi$ .

However, the above statement and Lemma 2 are capable of intersection detection for case 1(b) only if edge  $e_{b1}$  exists. Considering the situation where  $\mathcal{R}_A$  and  $\mathcal{R}_B$  are developed from different directions and  $T_k$  is the target position of  $\mathcal{R}_B$ , the case has to be reformulated as in Fig. B.16 and Lemma 2s.

**Lemma 2s** If edge  $e_{b1}$  does not exist, and node  $T_k$  is goal node of  $\mathcal{R}_B$ .  $\mathcal{R}_A$  and  $\mathcal{R}_B$  intersect at  $T_k$  if and only if clockwise (counterclockwise) angle from  $e_{a1}$  to  $e_{fc}$  is  $> \pi$  and the clockwise (counterclockwise) angle from  $e_{lc}$  to  $e_{b2}$  is  $> \pi$ .

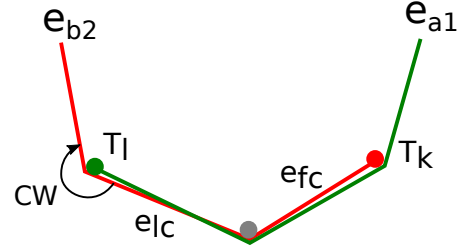


**Fig. B.16.** Case 1(b) supplement. Edge  $e_{b1}$  does not exist, meaning node  $T_k$  is goal node of  $\mathcal{R}_B$ .  $\mathcal{R}_A$  and  $\mathcal{R}_B$  intersect at  $T_l$ .

##### Appendix B.1.2. Case 2(b)

**Case 2(b):** Suppose  $\mathcal{R}_A$  and  $\mathcal{R}_B$  meet at node  $T_k$ , and each route has two edges incident to  $T_k$ . They share one of the edges. Let  $\mathcal{R}_A$  be the route currently in construction and  $\mathcal{R}_B$  be a previously constructed route.

In [8], this case is concluded as the following:

The edges and nodes labeling follow the convention in case 1(b), and an edge  $e_{a2}$  of  $\mathcal{R}_A$  is added immediately after the common set of edges. An illustration is shown in Fig. B.17. Assume that the edge  $e_{b2}$  is in the counterclockwise angle from  $e_{a2}$  to  $e_{lc}$ . Then Lemma 4 is used to determine intersection.

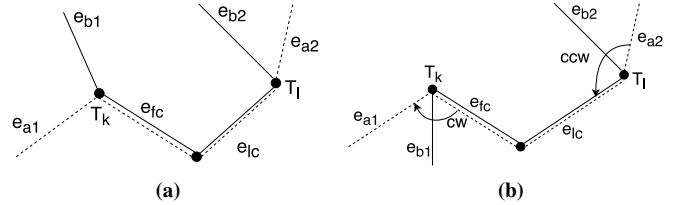


**Fig. B.17.** Case 2(b). In both (a) and (b)  $\mathcal{R}_A$  and  $\mathcal{R}_B$  intersect at node  $T_k$ . (The figure is taken from [8] Fig. 14.)

**Lemma 4**  $\mathcal{R}_A$  and  $\mathcal{R}_B$  intersect at  $T_k$  if and only if (a)  $e_{b1}$  is contained in the concave angle between  $e_{a1}$  and  $e_{fc}$  and  $e_{a1}$  is contained in the concave angle between  $e_{b1}$  and  $e_{fc}$  or (b)  $e_{b1}$  is contained in the clockwise angle from  $e_{fc}$  to  $e_{a1}$ .

However, the algorithm is redundant for option (a) in Lemma 4. Since the cable configuration is constructed in a depth-first manner, there is no need to proceed further if intersection has already been detected. Hence, it can be re-formulated as in Fig. B.18.

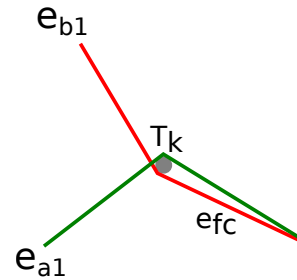


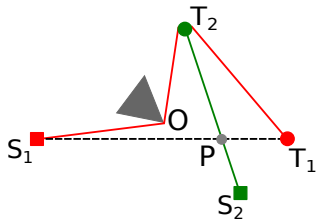
**Fig. B.18.** Revised Case 2(b) for Lemma 4(a).

In addition, option (b) in Lemma 4 only satisfy the situation when edge  $e_{b2}$  exists (recall the discussion for case 1(b)). When  $T_l$  is the goal node for  $\mathcal{R}_B$ , meaning there is no edge  $e_{b2}$ , Lemma 4(b) has to be revised. Below we present the revised version of Lemma 4.

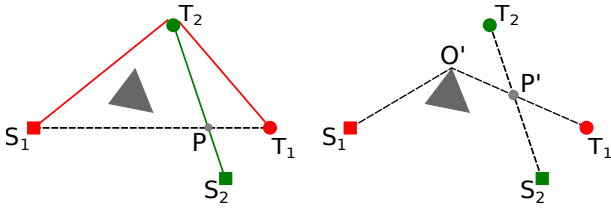
**Lemma 4r**  $\mathcal{R}_A$  and  $\mathcal{R}_B$  intersect at  $T_k$  if and only if (a)  $e_{b1}$  is contained in the concave angle between  $e_{a1}$  and  $e_{fc}$  and  $e_{a1}$  is contained in the concave angle between  $e_{b1}$  and  $e_{fc}$ ; or (b1)  $e_{b1}$  is contained in the clockwise (counterclockwise) angle from  $e_{fc}$  to  $e_{a1}$  and edge  $e_{b2}$  is in the counterclockwise (clockwise) angle from  $e_{a2}$  to  $e_{lc}$ ; or (b2)  $e_{b1}$  is contained in the clockwise (counterclockwise) angle from  $e_{fc}$  to  $e_{a1}$  and counterclockwise (clockwise) angle from  $e_{a2}$  to  $e_{lc}$  is  $< \pi$  when  $T_l$  is the goal node for  $\mathcal{R}_B$ .

### Appendix C. Extension to workspace with obstacles

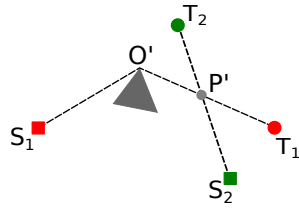
An obstacle interferes in robot's motion only when the whole piece or part of it is in the robot's cable polygon. An example is given in Fig. C.19.



(a) The obstacle is out of  $\Pi_1$  and  $\Pi_2$ . The target cable configuration can be achieved by straight-line robot motion as long as  $r_1$  passes point  $P$  before  $r_2$  does.



(b) The obstacle is in  $\Pi_1$ . The target cable configuration cannot be achieved if  $r_1$  moves along  $(S_1, T_1)$ .



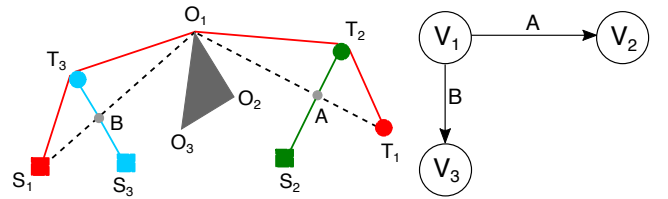
(c) The shortest paths for the robots for the case in (b). To achieve the target cable configuration,  $r_1$  has to move along  $S_1 - O' - P' - T_1$  and passes  $P'$  before  $r_2$  does.

**Fig. C.19.** Interference in robot's motion from the obstacle that is located in and out of robot's retraction polygon.

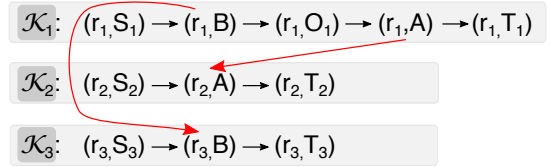
In Fig. C.19(a), the obstacle is located in the exterior of a robot's cable polygon. Although cable line  $C_1$  wraps around the obstacle at point  $O$  in the target cable configuration,  $r_1$  and  $r_2$  can still move along their  $(S, T)$  straight-line path to achieve the target cable configuration as long as  $r_1$  passes point  $P$  before  $r_2$  does, which behaves the same as the case without obstacles. By contrast, robot's path needs to be modified when the obstacle is (partially) in the interior of the robot's cable polygon. As

depicted in Fig. C.19(b, c), to achieve the target cable configuration, the shortest path for  $r_1$  is  $S_1 - O' - P' - T_1$ , and  $r_1$  must pass  $P'$  earlier than  $r_2$ .

The proposed algorithms for Straight/Concurrent motion can be adapted easily to the situation where there are obstacles in the workspace. The only modification is the robots' paths. Recall that the motivation to adopt straight-line motion is that it is the shortest path for a robot to reach its target position. When there are obstacles in the workspace, the shortest path of a robot is no longer its  $(S, T)$  straight-line segment, but its retracted cable line after all other robots are removed from the environment. The algorithms for Straight/Concurrent motion still hold for workspace with obstacles with the updated shortest paths. An example is presented in Fig. C.20.



(a) A given target cable configuration in the workspace with obstacles. (b) PIG of the target cable configuration.



(c) NIG of the target cable configuration with updated robot motion path.

**Fig. C.20.** An implementation of the proposed algorithms for the case where the workspace contains obstacles.

### References

### References

- [1] A. A. Nassiraei, Y. Kawamura, A. Ahrary, Y. Mikuriya, K. Ishii, Concept and design of a fully autonomous sewer pipe inspection mobile robot" kantaro", in: Robotics and Automation, 2007 IEEE International Conference on, IEEE, 2007, pp. 136–143.
- [2] D. Hong, S. A. Velinsky, K. Yamazaki, Tethered mobile robot for automating highway maintenance operations, Robotics and Computer-Integrated Manufacturing 13 (4) (1997) 297–307.
- [3] X. Zhang, M. Li, J. H. Lim, Y. Weng, Y. W. D. Tay, H. Pham, Q.-C. Pham, Large-scale 3d printing by a team of mobile robots, Automation in Construction 95 (2018) 98–106.
- [4] K. S. Pratt, R. R. Murphy, J. L. Burke, J. Craighead, C. Griffin, S. Stover, Use of tethered small unmanned aerial system at berkman plaza ii collapse, in: Safety, Security and Rescue Robotics, 2008. SSR 2008. IEEE International Workshop on, IEEE, 2008, pp. 134–139.
- [5] N. Michael, S. Shen, K. Mohta, Y. Mulgaonkar, V. Kumar, K. Nagatani, Y. Okada, S. Kiribayashi, K. Otake, K. Yoshida, K. Ohno, E. Takeuchi, S. Tadokoro, Collaborative mapping of an earthquake-damaged building via ground and aerial robots, Journal of Field Robotics 29 (5) (2012) 832–841.
- [6] S. Cass, Darpa unveils atlas drc robot, <https://spectrum.ieee.org/automaton/robotics/humanoids/darpa-unveils-atlas-drc-robot> (2013).

- [7] P. McGarey, F. Pomerleau, T. D. Barfoot, System design of a tethered robotic explorer (trex) for 3d mapping of steep terrain and harsh environments, in: *Field and Service Robotics*, Springer, 2016, pp. 267–281.
- [8] S. Hert, V. Lumelsky, Planar curve routing for tethered-robot motion planning, *International Journal of Computational Geometry & Applications* 7 (03) (1997) 225–252.
- [9] R. Siegwart, I. R. Nourbakhsh, D. Scaramuzza, R. C. Arkin, *Introduction to autonomous mobile robots*, MIT press, 2011.
- [10] S. Hert, V. Lumelsky, The ties that bind: Motion planning for multiple tethered robots, in: *Robotics and Automation, 1994. Proceedings.*, 1994 IEEE International Conference on, IEEE, 1994, pp. 2734–2741.
- [11] S. Hert, V. Lumelsky, The ties that bind: Motion planning for multiple tethered robots, *Robotics and Autonomous Systems* 17 (3) (1996) 187 – 215.
- [12] P. G. Xavier, Shortest path planning for a tethered robot or an anchored cable, in: *Robotics and Automation, 1999. Proceedings.* 1999 IEEE International Conference on, Vol. 2, IEEE, 1999, pp. 1011–1017.
- [13] N. Xu, P. Brass, I. Vigan, An improved algorithm in shortest path planning for a tethered robot, 2012.
- [14] T. Igarashi, M. Stilman, Homotopic path planning on manifolds for cabled mobile robots, in: *Algorithmic Foundations of Robotics IX*, Springer, 2010, pp. 1–18.
- [15] S. Kim, S. Bhattacharya, V. Kumar, Path planning for a tethered mobile robot, in: *Robotics and Automation (ICRA), 2014 IEEE International Conference on*, IEEE, 2014, pp. 1132–1139.
- [16] S. Kim, M. Likhachev, Path planning for a tethered robot using multi-heuristic a\* with topology-based heuristics, in: *Intelligent Robots and Systems (IROS), 2015 IEEE/RSJ International Conference on*, IEEE, 2015, pp. 4656–4663.
- [17] S. Bhattacharya, S. Kim, H. Heidarsson, G. S. Sukhatme, V. Kumar, A topological approach to using cables to separate and manipulate sets of objects, *The International Journal of Robotics Research* 34 (6) (2015) 799–815.
- [18] O. Salzman, D. Halperin, Optimal motion planning for a tethered robot: Efficient preprocessing for fast shortest paths queries, in: *Robotics and Automation (ICRA), 2015 IEEE International Conference on*, IEEE, 2015, pp. 4161–4166.
- [19] R. H. Teshnizi, D. A. Shell, Computing cell-based decompositions dynamically for planning motions of tethered robots, in: *2014 IEEE International Conference on Robotics and Automation (ICRA), IEEE, 2014*, pp. 6130–6135.
- [20] R. H. Teshnizi, D. A. Shell, Planning motions for a planar robot attached to a stiff tether, in: *2016 IEEE International Conference on Robotics and Automation (ICRA), IEEE, 2016*, pp. 2759–2766.
- [21] I. Shnaps, E. Rimon, Online coverage by a tethered autonomous mobile robot in planar unknown environments, *IEEE Transactions on Robotics* 30 (4) (2014) 966–974.
- [22] P. Abad-Manterola, I. A. Nesnas, J. W. Burdick, Motion planning on steep terrain for the tethered axel rover, in: *Robotics and Automation (ICRA), 2011 IEEE International Conference on*, IEEE, 2011, pp. 4188–4195.
- [23] M. M. Tanner, J. W. Burdick, I. A. Nesnas, Online motion planning for tethered robots in extreme terrain, in: *Robotics and Automation (ICRA), 2013 IEEE International Conference on*, IEEE, 2013, pp. 5557–5564.
- [24] P. McGarey, K. MacTavish, F. Pomerleau, T. D. Barfoot, The line leading the blind: Towards nonvisual localization and mapping for tethered mobile robots, in: *2016 IEEE International Conference on Robotics and Automation (ICRA), IEEE, 2016*, pp. 4799–4806.
- [25] P. McGarey, K. MacTavish, F. Pomerleau, T. D. Barfoot, Tslam: Tethered simultaneous localization and mapping for mobile robots, *The International Journal of Robotics Research* 36 (12) (2017) 1363–1386.
- [26] P. McGarey, M. Polzin, T. D. Barfoot, Falling in line: Visual route following on extreme terrain for a tethered mobile robot, in: *2017 IEEE International Conference on Robotics and Automation (ICRA), IEEE, 2017*, pp. 2027–2034.
- [27] D. Tsai, I. A. Nesnas, D. Zanzhitzky, Autonomous vision-based tethered-assisted rover docking, in: *2013 IEEE/RSJ International Conference on Intelligent Robots and Systems*, IEEE, 2013, pp. 2834–2841.
- [28] A. Yamashita, J. Sasaki, J. Ota, T. Arai, Cooperative manipulation of objects by multiple mobile robots with tools, in: *Proceedings of the 4th Japan-France/2nd Asia-Europe Congress on Mechatronics*, Vol. 310, 1998, p. 315.
- [29] S. Bhattacharya, H. Heidarsson, G. S. Sukhatme, V. Kumar, Cooperative control of autonomous surface vehicles for oil skimming and cleanup, in: *Robotics and automation (ICRA), 2011 IEEE international conference on*, IEEE, 2011, pp. 2374–2379.
- [30] S. Khuller, E. Rivlin, A. Rosenfeld, Graphbots: cooperative motion planning in discrete spaces, *IEEE Transactions on Systems, Man, and Cybernetics, Part C (Applications and Reviews)* 28 (1) (1998) 29–38.
- [31] S. Hert, V. Lumelsky, Motion planning in  $\mathbb{R}^3$  for multiple tethered robots, *IEEE transactions on robotics and automation* 15 (4) (1999) 623–639.
- [32] F. Sinden, The tethered robot problem, *The international journal of robotics research* 9 (1) (1990) 122–133.
- [33] T. C. Hales, Jordan’s proof of the jordan curve theorem, *Studies in logic, grammar and rhetoric* 10 (23) (2007) 45–60.